Effect of RNA Secondary Structure on RNA Cleavage Catalyzed by HIV-1 Reverse Transcriptase†

Zucai Suo and Kenneth A. Johnson*

Department of Biochemistry and Molecular Biology, 106 Althouse Laboratory, The Pennsylvania State University, University Park, Pennsylvania 16802

Received May 23, 1997; Revised Manuscript Received July 29, 1997⊗

ABSTRACT: Using a synthetic 66 nucleotide RNA template containing a stable hairpin structure derived from the HIV-1 genome, six predominant RNA cleavage products are found during DNA synthesis catalyzed by HIV-1 RT. These major RNA cleavage sites correlate well with the pause sites seen during primer elongation [Suo, Z., & Johnson, K. A. (1997) *Biochemistry* (manuscript submitted for publication)]. Thus, the RNase H and polymerase activities of RT are coupled as RT reads through the RNA secondary structure. The distance between the two active sites of HIV-1 RT is 19−20 base pairs of DNA/RNA heteroduplex when the next template base is not paired. The heteroduplex region was enlarged by 2−3 base pairs once RT encounters the template hairpin. A model for this change is presented. At the pause sites, the burst amplitudes of RNA cleavage are larger than the corresponding reaction amplitudes of next nucleotide incorporation at the polymerase site. Measurement of the steady state rates of RNA cleavage confirms that all substrates dissociate slowly from RT. These results suggest that while substrates are bound nonproductively at the polymerase site, they are still bound productively at the RNase H active site of RT. Characterization of an RNase H-deficient RT mutant (D443N) shows that RNase H activity is not critical for RT to read through the RNA secondary structure. HIV-1 nucleocapsid does not increase the processivity of HIV-1 RT but inhibits DNA elongation by blocking the binding of RT to DNA substrates.

Human immunodeficiency virus 1 (HIV-1)[1] reverse transcriptase (RT) is a heterodimer of two polypeptides (p66 and p51). RT has polymerase and RNase H activities, which reside on the p66 subunit (Hansen *et al.*, 1987). The RNase H activity is required at several stages of viral replication, including degradation of the viral RNA after minus-strand DNA synthesis, generation of a specific oligopurine ribonucleotide primer for plus-strand DNA synthesis, and subsequent removal of the oligopurine primer (Champoux, 1993).

The fact that the RNase H and polymerase sites of HIV-1 RT reside on the same polypeptide chain suggests a possible coupling between RNA cleavage and DNA synthesis. While some data (Schatz *et al.*, 1990; Wöhrl & Moelling, 1990; Furfine & Reardon, 1991) support such a coupling, other evidence supports an uncoupled mechanism (Huber et al., 1989; Kati *et al.*, 1992; DeStefano *et al.*, 1991). There is also some controversy about the distance between the two active sites of RT. This distance has been estimated to be 15−16 base pairs (Furfine & Reardon, 1991) or 19 base pairs (Kati *et al.*, 1992), while the crystal structure with DNA bound shows an 19−20 base pair distance (Kohlstaedt *et al.*, 1992; Jacobo-Molina *et al.*, 1993). Additionally, the HIV-1 RNA genome forms complex secondary and tertiary structures. We have demonstrated that RNA secondary structure stalls HIV-1 RT and affects its DNA polymerase activity (Suo & Johnson, 1997a,b).

HIV-1 RT copies both DNA and RNA *in vitro* with low processivity (∼10−300 nucleotides; Kati *et al.*, 1992; Klarmann *et al.*, 1993). This low processivity is very unusual for a replicative enzyme and suggests that HIV-1 RT, like other replicative DNA polymerases, may function in coordination with one or more accessory proteins provided by either virus or host during viral DNA synthesis *in vivo*. HIV-1 nucleocapsid protein (nucleocapsid), which is an abundant viral core protein, is a possible accessory protein. Nucleocapsid binds to the viral tRNA by virtue of its affinity for single-stranded RNA and unwinds tRNA to stimulate its annealing to the viral RNA template to form the initiation complex (Khan & Giedroc, 1992; You *et al.*, 1993).

In this report, we examine how RNA secondary structure affects the RNase H activity, the distance between the two active sites of HIV-1 RT, and the possible coupling between them. We used the same 66 nucleotide RNA template as in Suo & Johnson (1997a,b) to examine the effect of RNA secondary structure on RNA cleavage catalyzed by RNase H activity of HIV-1 RT *in vitro*. The possible role of RNase H activity of RT on the melting of RNA secondary structure was determined. The possible accessory proteins, including HIV-1 nucleocapsid, RNA helicases from HeLa cells, T7 DNA helicase, and *Escherichia coli* thioredoxin, were also tested for their effect on the processivity of HIV-1 RT.

MATERIALS AND METHODS

Construction of p66(D443N). Mizrahi *et al.* (1990) reported that when aspartate 443 was replaced with an asparagine in HIV-1 RT, the resulting enzyme (D443N) was

† This work is supported by National Institutes of Health Grant GM44613 (to K.A.J.).

* Author to whom correspondence should be addressed. Tel: (814) 865-1200. Fax: (814) 865-3030. Email: kaj1@psu.edu.

⊗ Abstract published in *Advance ACS Abstracts,* September 15, 1997.

[1] Abbreviations: bp, base pair; cpm, counts per minute; dNTP, 2′-deoxynucleotide 5′-triphosphate; HIV-1, human immunodeficiency virus type 1; RNase, ribonuclease; RT, reverse transcriptase; wt, wild-type.

S0006-2960(97)01218-X CCC: $14.00

defective in RNase H function, but exhibited wild-type polymerase activity. Plasmid pRT_{66} containing the gene encoding the wild-type 66 kDa subunit was provided by Dr. Roger S. Goody (Muller *et al.*, 1989). We inserted the mutation into pRT_{66} using the transformer site-directed mutagenesis kit (Clontech), according to manufacturer's instructions. The D443N mutation was confirmed by dideoxy DNA sequencing (Sanger *et al.*, 1977). The mutagenized portion of pRT_{66} was then excised as a 328 bp *Kpn*I fragment from nucleotides 1277 to 1605. The mutated 328 bp fragment was ligated into a wild-type pRT_{66}, from which the wild-type 328 bp *Kpn*I fragment had been removed. This construct was transformed into *E. coli* strain JM109. Correctly constructed plasmids were determined by restriction enzyme digestion and dideoxy DNA sequencing. Finally, the mutagenized plasmid mut-pRT_{66} was transformed into expression cell line *E. coli* 6222/pDMI,1. The previously prepared expression cell line *E. coli* 6222/pDMI,1 containing the plasmid (pRT_{51}) encoding wild-type p51 subunit was provided by R. S. Goody.

Protein Expression and Purification. The two cell lines producing the p66(D443N) and wild-type p51 subunits were grown separately in Luria Broth media containing ampicillin (0.1 mg/mL) at 37 °C. The cells were induced by the addition of 0.5 mM isopropyl β-D-thiogalactopyranoside when the absorbance at 600 nm of cell culture reached 0.4. After induction, the cells were grown for 6 h at 37 °C. The cells were harvested separately. The two cell pellets were resuspended separately in a buffer which contained 50 mM Tris-Cl, pH 7.9, 2 mM EDTA, 2 mM DTT, 10% glycerol, 0.5 M NaCl, and 1 mM phenylmethanesulfonyl fluoride. The cell paste containing p66 (D443N) and the cell paste containing p51 were combined in a ratio of 1:1 by weight. The RT mutant D443N was purified by following the same purification procedure described in the preceding article in this issue (Suo & Johnson, 1996a). The ratio of the Coomassie Blue staining intensities of two bands suggested a final subunit composition of 1.31:1.00 (66/51 kDa). The enzyme concentration was determined spectrophotometrically by using an extinction coefficient of 260 450 M^{-1} cm^{-1} for the mutant RT heterodimer at 280 nm. All concentrations of RT reported in this paper were determined spectrophotometrically.

The pre-steady-state kinetics of incorporation of dATP to the 25/45-mer DNA/DNA duplex suggests that the purified D443N is about 70% active and is very similar to wild-type RT in polymerase activity but lacks the RNase H activity. No RNA cleavage products were observed after 25/66-mer DNA/RNA duplex was incubated with D443N in the presence of 10 mM Mg^{2+} at 37 °C for 30 min (data not shown).

E. coli thioredoxin was purchased from Promega (Madison, WI). HIV nucleocapsid protein (NCp7) was a generous gift from Dr. Charles S. McHenry. RNA helicase A and II from HeLa cells were kindly provided by Dr. Jerard Hurwitz. T7 DNA helicase (Patel *et al.*, 1992) were overexpressed and purified by Dr. Kevin Hacker in our lab.

Synthetic Oligonucleotides. The 66 nucleotide RNA template was synthesized by runoff transcription by T7 RNA polymerase, and then annealed to synthetic oligonucleotide DNA primers as described by Suo and Johnson (1997a). It should be noted that RNA templates longer than 66 by 1 or 2 nucleotides can be seen in Figure 1. These 67 and 68 nucleotide templates are the products of blunt end incorporations during synthesis using the T7 runoff transcription method. They did not affect the experiments because they have the same 5′ termini as 66-mer.

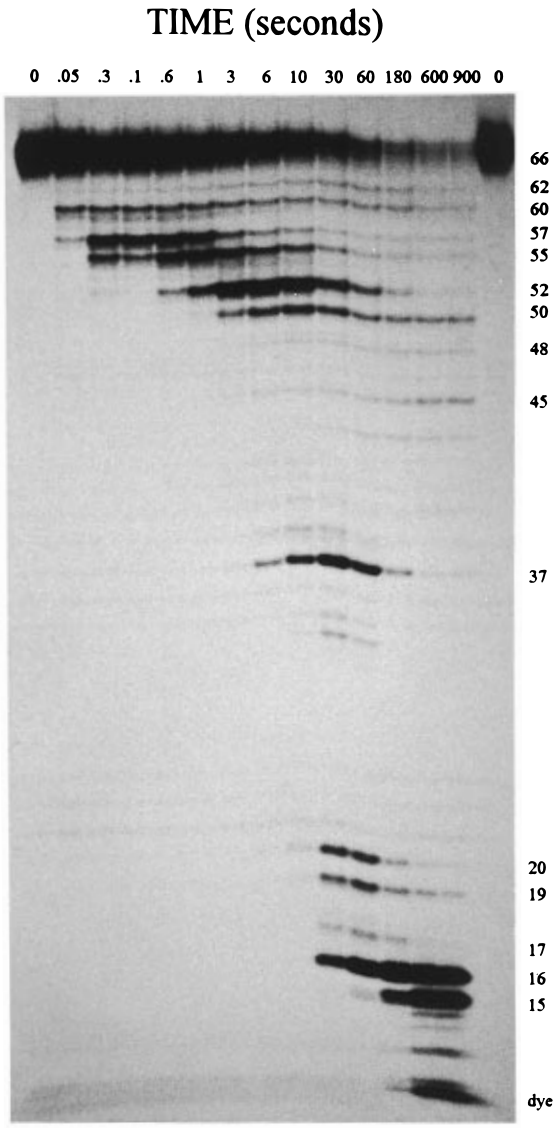

FIGURE 1: RNA cleavage during DNA polymerization. A solution of RT (100 nM) was incubated with DNA/RNA 25/66-mer (100 nM, 66-mer was 5′ ^{32}P-labeled) and then reacted with dATP, dGTP, dCTP, and dTTP (150 μM each) in Mg^{2+} buffer (pH 7.5). The reactions were quenched with 0.3 M EDTA (final concentrations) at the indicated times and analyzed by sequencing gel electrophoresis. The size of cleavage products was determined by enzymatic RNA sequencing. The reaction was performed using wild-type HIV-1 RT at 37 °C.

Enzymatic Sequencing the RNA 66-Mer. RNA 66-mer was enzymatically sequenced using RNase T1, U2 and *B. cereus* (Pharmacia), and RNase CL3 (Boehringer Mannheim). The 5′ ^{32}P-labeled RNA 66-mer (0.25 pmol, 10^6 cpm) incubated in buffer containing 10 μg of carrier tRNA (Sigma) was heated for 10 min at 55 °C. Then one of the following RNases was added and incubated at 55 °C for 12 min: 1.0 unit of RNase T1, 2 units of RNase U2, 0.2 unit of RNase CL3, or 2 units of RNase *B. cereus*. T1 buffer consists of 33 mM sodium citrate (pH 5.0), 1 mM EDTA, and 7.5 M urea. U2 buffer has the same composition as the T1 buffer except that the pH is 3.5. CL3 buffer has 10 mM Tris-Cl (pH 8.0), 2.0 mM EDTA, and 7.5 M urea. *B. cereus* buffer

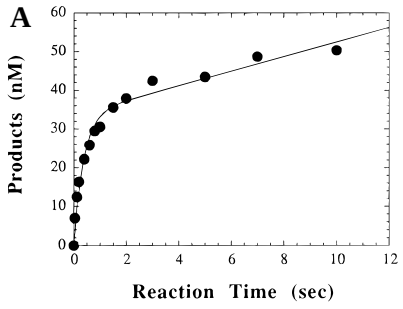

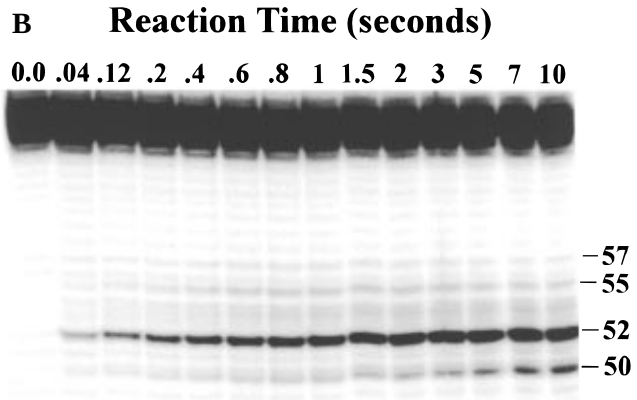

FIGURE 2: Pre-steady-state kinetics of RNA cleavage. A solution of wt-RT (100 nM) was incubated with 35/66-mer (200 nM, RNA was 5′ ^{32}P-labeled) and then mixed with dGTP (100 μM) plus Mg^{2+} (10 mM) (final concentrations) to start the reaction at 37 °C. The reactions were quenched by the addition of 0.3 M EDTA and RNA cleavage products were quantitated by sequencing gel analysis. The data were fitted to a burst equation, which gave a burst rate of 2.64 s^{-1}, a steady state rate of 0.056 s^{-1} and a burst amplitude of 33.6%.

has 33 mM sodium citrate (pH 5.0) and 1 mM EDTA. Alkaline hydrolysis of 0.5 pmol of 5′ ^{32}P-labeled RNA 66-mer (2×10^6 cpm) occurred in 0.15 M $NaHCO_3$, 0.15 M Na_2CO_3, 1 mM EDTA, pH 9.2, and 5 μg of carrier tRNA at 90 °C for 6 min.

RESULTS

RNA Cleavage during DNA Elongation Catalyzed by Wt-RT at 37 °C. To examine how RNA secondary structure affects the RNase H activity of RT during concomitant DNA synthesis, we performed the experiment described in Figure 2 of Suo & Johnson (1997b) but with the RNA template 5′-radiolabeled. A solution of wt-RT was incubated with 25/66-mer and then mixed with the four dNTPs in Mg^{2+} containing buffer (Suo & Johnson, 1997a) to start the reaction. The reactions were then quenched with 0.3 M EDTA at times indicated. The RNA cleavage products were analyzed by a 12% sequencing gel as shown in Figure 1. The sizes of the accumulated RNA products were determined by performing enzymatic RNA sequencing reactions and then analyzing the sequencing reaction products along with the RNA cleavage products on the same sequencing gel (data not shown). The predominant RNA products are 62, 60, 57, 55, 52, 50, 37, 20, 19, 17, 16, and 15 nucleotides in length while the minor products are 48, 45, 43, 35, and 34 nucleotides in length. The RNA cleavage continued after the DNA synthesis stopped. This experiment was also performed at 8 and 21 °C (data not shown); the patterns of RNA product accumulation at 8, 21, and 37 °C are similar except that the same RNA products appeared more intensely at longer reaction times at the lower reaction temperatures due to less extensive hydrolysis. For example, the RNA cleavage was very slow at 8 °C because there was almost no RNA cleavage product shorter than 37 nucleotides even after 30 min at 8 °C. The remainder of the analysis described in this report was performed at 37 °C.

Table 1: Pre-Steady-State Kinetic Constants of RNA Cleavage[a]

substrate	burst rate (s^{-1})	burst amplitude (%)	steady state rate (s^{-1})
25/66-mer	5.04 ± 0.75	55.7 ± 1.9	0.036 ± 0.006
32/66-mer	2.15 ± 0.14	40.2 ± 1.1	0.054 ± 0.006
35/66-mer	2.64 ± 0.38	33.6 ± 1.8	0.056 ± 0.012
36/66-mer	1.66 ± 0.19	30.8 ± 1.9	0.039 ± 0.012
37/66-mer	0.67 ± 0.02	56.0 ± 1.4	0.014 ± 0.003
48/66-mer	6.20 ± 0.92	70.8 ± 2.7	0.039 ± 0.009

[a] The substrates corresponding to the strong pause sites are in bold-type.

Pre-Steady-State Kinetics of RNA Cleavage Catalyzed by wt-RT. In the previous article in this issue, we showed that a large portion of RNA templates were not bound productively at the polymerase site of RT but still bound tightly to RT (Suo & Johnson, 1997a). More importantly, the nonproductively bound DNA/RNA duplex could be converted to a productive binding mode without dissociation from the enzyme. To test whether the RNase H site of RT bound the RNA template when DNA synthesis was stalled at the pause sites, we performed pre-steady-state kinetic analysis of RNA cleavage during single nucleotide incorporation. This analysis was conducted under conditions in which the DNA/RNA duplex was in slight excess relative to the RT concentration. The reaction was initiated by mixing a solution containing the complex of wt-RT and 35/66-mer with a solution of dGTP (the next correct nucleotide) in Mg^{2+} buffer (Suo & Johnson, 1997a). The RNA 66-mer was 5′ radiolabeled and the 35-mer primer was complementary to the 3′ terminus of 66-mer. The reaction was quenched with 0.3 M EDTA at time intervals ranging from 40 ms to 10 s. The 52-mer was the major product while small amounts of 50, 55, and 57-mer also formed (Inset of Figure 2). The time course of formation of all cleavage products shows a burst followed by a linear slow phase (Figure 2). The data were fitted to a burst equation to get the kinetic constants shown in Table 1.

Similar pre-steady-state kinetic analyses of RNA cleavage were conducted with other DNA primers: 25, 35, 36, 37, and 48mer (all complementary to the 3′ terminus of 66-mer). In each case, there was one major cleavage product and several minor products for each DNA/RNA duplex. Each resulting time course of RNA cleavage was fitted to a burst equation with a fast exponential phase followed by a linear phase. The kinetic data obtained for each primer are summarized in Table 1. The burst rates and reaction amplitudes vary with different substrates but the steady state rates are all in the same range (0.04 ± 0.01 s^{-1}). The steady state rate is limited by the rate of dissociation of the DNA/RNA duplex from the enzyme.

Determination of the Distance between the Dominant RNA Cleavage Site and the 3′ Terminus of Primer. If we can determine the relationship between the RNA products and the DNA products which accumulate during processive synthesis through the hairpin, we can estimate the distance

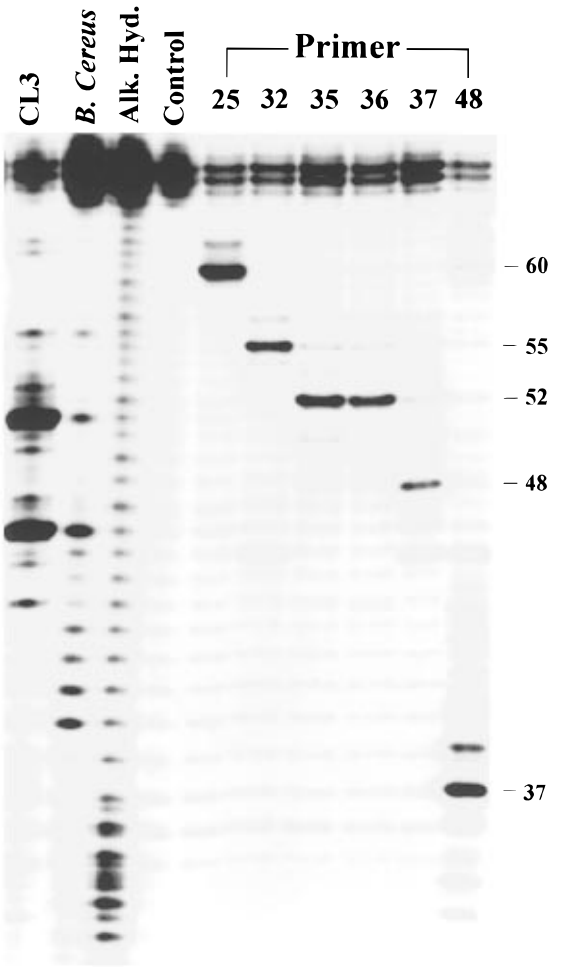

FIGURE 3: RNA cleavage pattern with various DNA primers. A solution of wt-RT (100 nM) was incubated with various DNA/RNA duplexes (200 nM, RNA was 5′ ^{32}P-labeled) and then mixed with Mg^{2+} (10 mM) (final concentrations) to start the RNase H reaction. The reactions were quenched by the addition of 0.3 M EDTA after 400 ms at 37 °C. The reaction was performed separately with 25/66-mer, 32/66-mer, 35/66-mer, 36/66-mer, 37/66-mer, and 48/66-mer substrates. The RNA cleavage products from each reaction were quantitated by sequencing gel analysis to obtain the results shown. The sizes of RNA products were determined by enzymatic RNA sequencing using RNase *B. cereus* and CL3. Lanes L and C denote the alkaline hydrolysis ladder and the control reaction without ribonuclease, respectively.

Table 2: Distances between the 3′ Termini of the DNA Primer and the Corresponding Major RNA Cleavage Site[a]

DNA primer (nucleotides)	25	**32**	**35**	**36**	37	**48**
RNA product (nucleotides)	60	55	52	52	48	37
distance (base pairs)	19	21	21	22	19	19

[a] The sizes of the DNA primers corresponding to the strong pause sites are in bold-type.

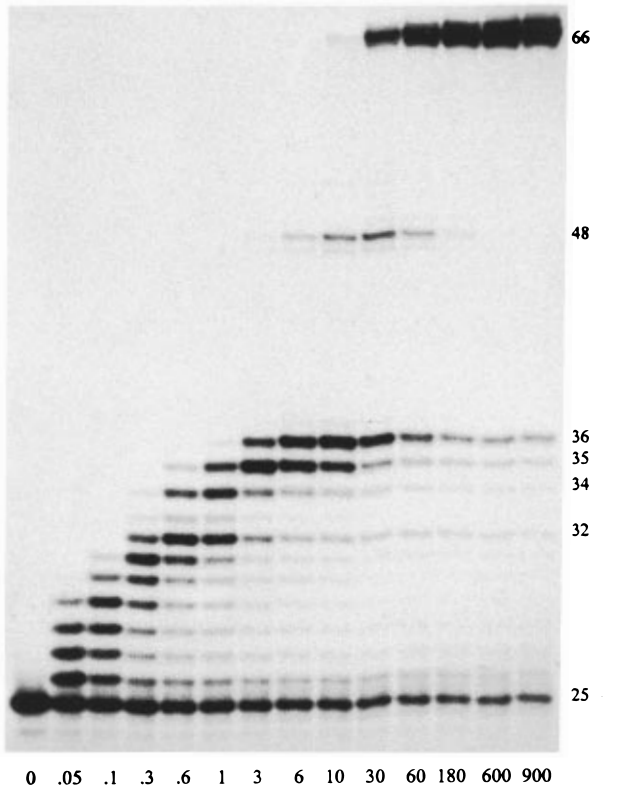

FIGURE 4: Processive polymerization catalyzed by RNase H-deficient RT mutant D443N. A solution of mut-RT (100 nM) was incubated with 5′ ^{32}P-labeled 25/66-mer DNA/RNA (100 nM) and was then reacted with dATP, dGTP, dCTP, and dTTP (150 μM each) in Mg^{2+} containing buffer at 37 °C. The reactions were quenched with 0.3 M EDTA (final concentrations) at the indicated times and analyzed by sequencing gel electrophoresis.

between the polymerase and RNase H active site at pause and nonpause sites. To accomplish this, we performed RNA cleavage while halting DNA synthesis. RNA cleavage in the absence of added nucleotides was conducted for 400 ms with different primers. Cleavage products were then analyzed on a sequencing gel (Figure 3). The reaction time of 400 ms was chosen as the time in which predominant RNA cleavage products were clearly visible and resulted from a single enzyme binding event. The major cleavage products 60, 55, 52, 52, 48, and 37-mer correspond to primers 25, 32, 35, 36, 37, and 48-mer, respectively (Table 2). Similar results from cleavage in the absence of dNTPs for 50 ms were obtained (data not shown). We also performed the 400 ms cleavage reaction in the presence of dNTPs, and the cleavage pattern at the strong pause sites is similar to the one in Figure 3 and the cleavage sites at nonpause sites changed due to fast incorporation of nucleotides (data not shown). These results demonstrate that there is a correlation between the DNA [Figure 2 of Suo and Johnson (1997b)] and RNA (Figure 1) product accumulation patterns. The distances between the cleavage sites observed with the various DNA primers vary from 19 to 22 base pairs as summarized in Table 2. We conclude that the RNA secondary structure may increase the distance between the polymerase site and the RNase H site by increasing the observed distance by 2−3 base pairs.

Processive Polymerization Catalyzed by RNase H-deficient RT. To test whether the RNase H domain alters the rate of DNA synthesis through the RNA template secondary structure, we performed the same processive polymerization experiment described in Figure 2 of Suo and Johnson (1997b), but with the RNase H deficient mutant D443N. A solution of the D443N mutant RT was incubated with 5′ ^{32}P-labeled DNA/RNA 25/66-mer and then was mixed with the four dNTPs in Mg^{2+} buffer for the indicated times prior to quenching with 0.3 M EDTA. The products of primer elongation were analyzed by sequencing gel electrophoresis. The results are shown in Figure 4. These results, obtained

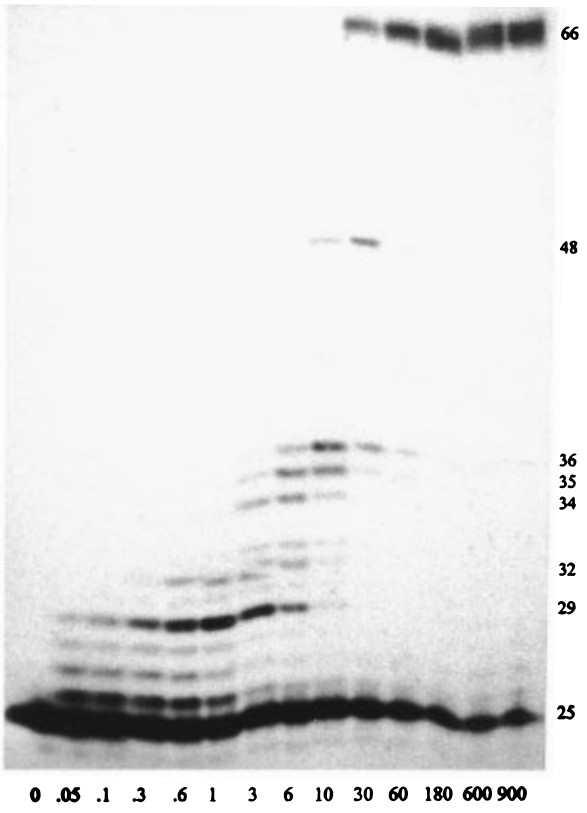

FIGURE 5: Effect of HIV-1 nucleocapsid protein (NCp7) on processive polymerization. A solution of wt-RT (100 nM) was incubated with 5′ ^{32}P-labeled 25/66-mer (100 nM), NCp7 (3 μM), and zinc acetate (150 μM) and was then mixed with dATP, dGTP, dCTP, and dTTP (150 μM each) (final concentrations) in Mg^{2+} containing buffer at 37 °C for the indicated times prior to quenching with 0.3 M EDTA. The products were then analyzed by sequencing gel electrophoresis.

using the RNase H-deficient mutant, are almost identical to those obtained with the wt-RT [see Figure 2 in Suo and Johnson (1997b)].

Effect of HIV Nucleocapsid and Several Other Proteins on Processivity of RT. The effect of mature nucleocapsid NCp7 on the processivity of HIV-1 RT was tested by similar processive polymerization experiments as in Figure 4. A preincubated solution of wt-RT, 25/66-mer, NCp7, and $ZnAc_2$ was allowed to react with four dNTPs in Mg^{2+} buffer for the indicated times prior to quenching with 0.3 M EDTA, and analysis by DNA sequencing gel. The results are shown in Figure 5. After the same reaction times, the full-length products were less while more starting primer 25-mer left than those in the absence of NCp7. The product accumulation pattern is similar to Figure 2 in Suo and Johnson (1997b) except that there was more accumulated 29-mer. Therefore, the NCp7 activity does not directly influence the progress of DNA polymerization while RT reads through the hairpin.

Similar processive polymerization experiments were performed to examine the role of possible accessory proteins RNA helicase A and II from Hela cells individually. Neither RNA helicase was found to have an effect on the processivity of RT (data not shown). We also tested T7 DNA helicase and *E. coli* thioredoxin individually with the DNA analog 66-mer as the template. No effect on the processivity of RT was observed (data not shown).

DISCUSSION

Coupling between RNA Cleavage and DNA Synthesis. RNA cleavage products accumulated (Figure 1) to produce a pattern that mirrored the pausing of DNA polymerization during processive synthesis through the RNA hairpin [Figure 2 in Suo and Johnson (1997b)]. For example, RNA cleavage stopped after the generation of an RNA 37-mer simultaneously with the pausing of DNA polymerization after formation of a 48-mer. The relationship between the accumulated RNA and DNA products was further defined by performing RNA cleavage for 400 ms in the absence of dNTPs with various primers at 37 °C (Figure 3). Each DNA primer correlates to a specific RNA cleavage product. These results demonstrate that there is coupling between RNA cleavage and DNA polymerization even in the presence of RNA secondary structure. This coupling has been previously reported (Schatz *et al.*, 1990; Wöhrl & Moelling, 1990; Furfine & Reardon, 1991), but the shorter time resolution reported here provides better definition of the initial cleavage site without the complications introduced by slower subsequent cleavage reactions.

Distance between the Polymerase and RNase H Active Sites of HIV-1 RT. The preferential RNA cleavage sites were all demonstrated to be within 19−22 nucleotides from the 3′ termini of DNA primers (Figure 3). This indicates that the RNase H and polymerase active sites of RT are spatially arranged such that they contact substrates at a certain range of distances from each other. If the distance between the two active sites of RT is estimated using the distances between the two 3′ termini of DNA primers and the correlated RNA cleavage products (Table 2), it will vary from 19 to 22 base pairs at the different positions relative to the RNA secondary structure. A spacing of 19 base pairs seems to be reasonable because it agrees with the footprinting and modeling results based on the crystal structure of RT (Kohlstaedt *et al.*, 1992; Jacobo-Molina *et al.*, 1993; Hermann *et al.*, 1994; Wöhrl *et al.*, 1995) and with the results obtained by Kati *et al.* (1992) using a linear RNA template and with results presented here for the segments containing linear template regions. The shorter distances of 15−16 base pairs reported by Furfine and Reardon (1991) is likely a function of continued hydrolysis during the longer time of incubation. This is supported by the appearance of the shorter RNA cleavage products including the 15-mer and 16-mer due to further RNA hydrolysis after DNA synthesis completed after 10−15 min (Figure 1). However, for spacing of 21−22 base pairs, HIV-1 RT has extended the distance between the polymerase and RNase H sites by 2−3 nucleotides when binding the substrates in the paused complex close to the RNA secondary structure. The X-ray crystal structure of HIV-1 RT (Kohlstaedt *et al.*, 1992; Jacobo-Molina *et al.*, 1993) has shown that both the palm subdomain of p66 subunit containing the polymerase active site and the RNase H domain of p66 subunit interact extensively with other domains of p66 and p51 subunits. Although there are changes in RT structure upon DNA binding (Patel *et al.*, 1995; Rodgers *et al.*, 1995), we believe that physical extension of the protein by 5−7 Å is unlikely at the pause sites with the DNA bound. We favor a model where the distance between the polymerase and RNase H sites may remain fixed, but the 3′ termini of DNA primers of substrates may move out of the polymerase active site.

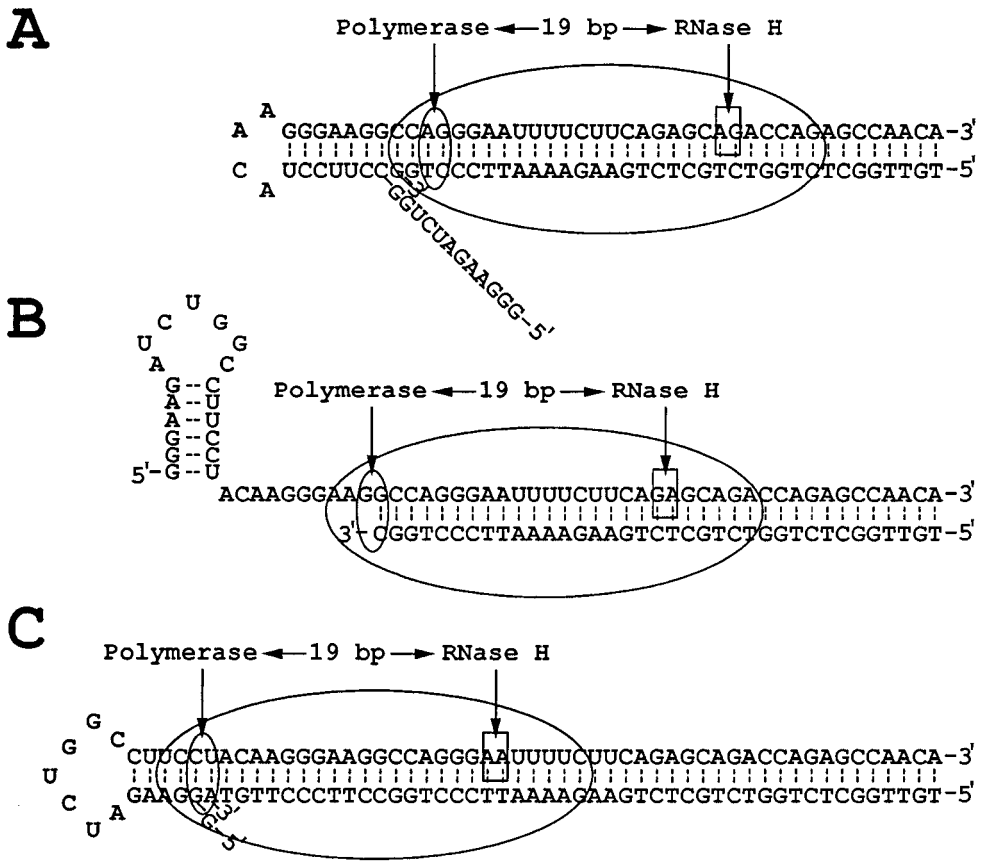

FIGURE 6: Structural models of RT binding to DNA/RNA. The large ellipses represent HIV-1 RT. The small ellipses and rectangles denote the polymerase and RNase H active sites, respectively. The DNA/RNA duplexes are (A) 36/66-mer, (B) 37/66-mer, and (C) 48/66-mer.

For example, the proposed model showing the binding of the 36/66-mer to RT in Figure 6A illustrates one possible scenario whereby the presence of the hairpin and the 5′ single-stranded tail force the polymerase back from the 3′ end by 3 base pairs such that the site of RNase H cleavage is now 22 base pairs from the 3′ terminus, although the distance between the polymerase and RNase H active sites remains fixed at 19 base pairs. This model may provide one reasonable explanation for the nonproductive binding observed at the pause sites during DNA polymerization (Suo & Johnson, 1997a). Accordingly, the distance between the two active sites of RT will remain fixed at 19 base pairs when RT is bound to the 32/66-mer, 35/66-mer, or 36/66−mer. Moreover, this model suggests that the protein may play a role in actively unwinding the RNA hairpin.

The distance between the polymerase and RNase H sites was estimated to be 19 base pairs with either 25/66-mer or 37/66-mer as the substrate. In substrate 25/66-mer, there is a single-stranded linker between the RNA secondary structure and the primer 25-mer and RT has not yet reached the hairpin structure (Suo & Johnson, 1997a). Similarly, there is a single-stranded region between the hairpin and the 3′ end of the primer in the substrate 37/66-mer resulting from the change in RNA secondary structure to form the smaller downstream hairpin (Suo & Johnson, 1997b). Therefore, both substrates were bound productively at the polymerase site as illustrated in Figure 6B. This interpretation is further supported by the observed tighter binding at the polymerase site of RT (Suo & Johnson, 1997a).

This simple model appears to be at odds with the observations of RNase H products formed while pausing at the 48-mer of DNA synthesis in that the spacing between the two active sites was also found to be 19 base pairs with 48/66-mer as the substrate. According to our model, this indicates that the 3′ terminus of the 48-mer was located very close to the polymerase site as illustrated in Figure 6C. The preceding paper in this issue demonstrated that this substrate was predominantly bound nonproductively to the polymerase site (Suo & Johnson, 1997a), presumably due to the large energy barrier for melting the GC base pair of the hairpin stem (Suo & Johnson, 1997b). The shorter observed distance between the polymerase and RNase H sites can be understood by comparison of Figure 6 A and C. In Figure 6A (36-mer), there are 12 nucleotides dangling on the 5′ end from the base of the hairpin, while in Figure 6C (48-mer), there is only one nucleotide. One nucleotide dangling on the 5′ end of the base of the hairpin in the 48/66-mer may not significantly affect the binding at the polymerase site of RT. In contrast, the 12 nucleotide dangling on the 5′ end of 36/66-mer at the base of the hairpin structure might have physical contact with the RT binding cleft and therefore significantly affect the binding of 36/66-mer at the polymerase site as shown in Figure 6A. This provides a rational explanation for the variation in distance between the major RNA cleavage sites and the 3′ terminus of DNA primer at the pause sites.

In conclusion, our data and the structural models suggest that the polymerase and RNase H sites of HIV-1 RT are separated by a fixed distance corresponding to 19 base pairs of DNA/RNA heteroduplex when RT transverses RNA secondary structure during replication. The observed distance (19 base pairs) between the 3′ terminus of DNA primer and the RNA cleavage site of 37/66-mer is very different from those of substrates with primers 32, 35, and 36-mer

Scheme 1

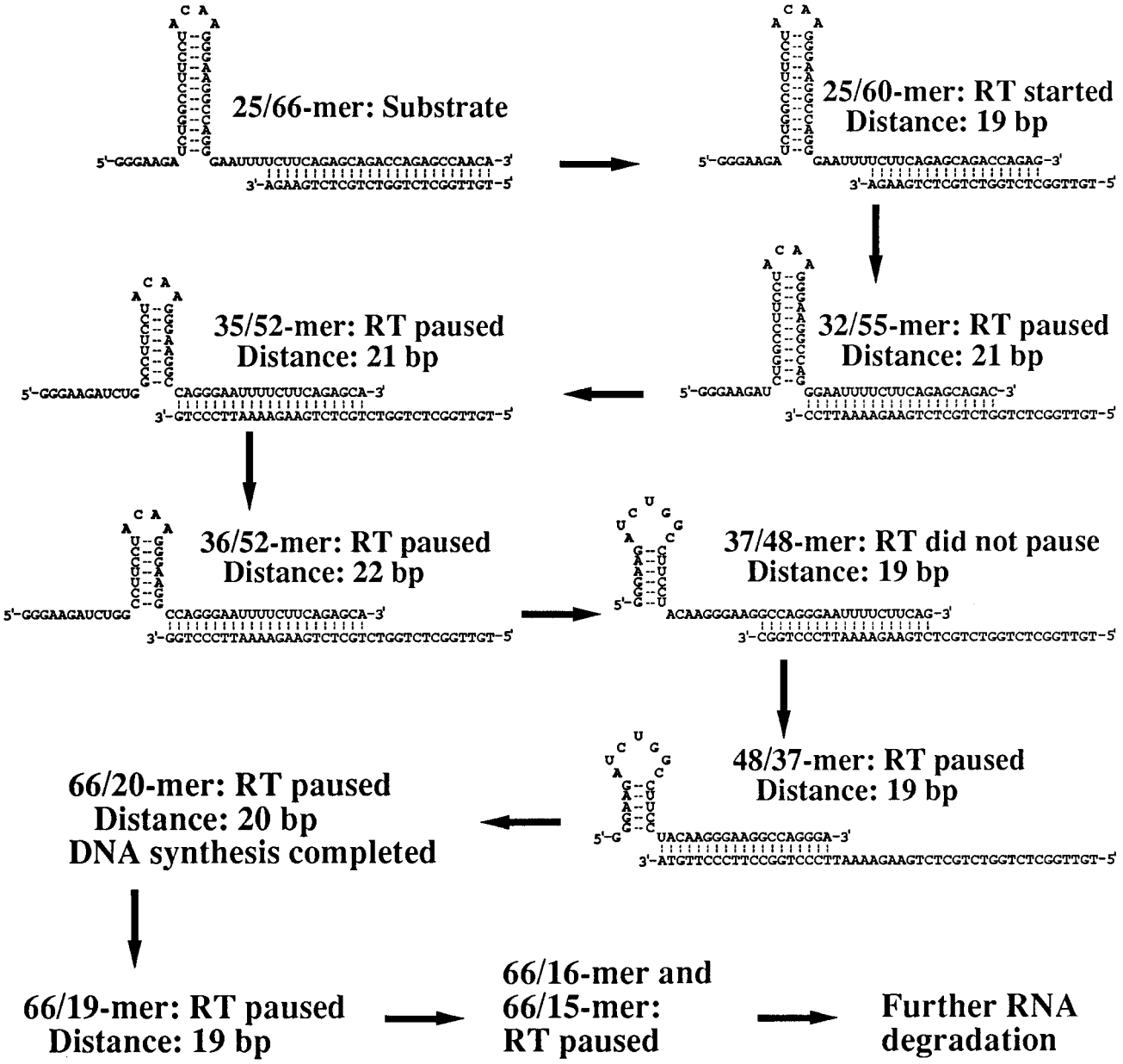

(21, 21, and 22 base pairs, respectively). This difference provides additional evidence for the RNA secondary structure change after synthesis of 37-mer (Suo & Johnson, 1997b).

On the basis of the results of Figures 1 and 3 as well as Figure 2 of Suo and Johnson (1997b), a model of RT traversing the RNA secondary structure at 37 °C is proposed (Scheme 1). Scheme 1 shows that RT paused at several sites during concomitant DNA polymerization and RNA cleavage. It also shows the change in RNA secondary structure and the further degradation of RNA template after completion of DNA synthesis. The distance between the 3′ terminus of DNA primer and the RNA cleavage site varies due to the effect of the RNA secondary structure as described above.

The RNA cleavage in the presence (Figure 2B) or absence (Figure 3) of dNTPs with different primers indicates that the RNA template was not sequentially cleaved from its 3′ terminus. Rather the RNase H of RT is an endonuclease, as described by Krug and Berger (1989). That the RNA template was further shortened to 15 and 16-mer after DNA elongation completed (Figure 1) suggests that the RNase H function of RT also has 3′ → 5′ exonuclease activity agreeing with results obtained by Schatz *et al.* (1990). However, the RNase H function of RT acts primarily as an endonuclease during DNA synthesis because the RNA cleavage is much slower than DNA polymerization and yet the two processes occur simultaneously.

Slow Dissociation of DNA/RNA Heteroduplex from RT. In the preceding paper in this issue, we determined that DNA substrates bind tightly to the polymerase site of RT and dissociate only slowly although the binding was largely nonproductive at pause sites (Suo & Johnson, 1997a). In this report, we show that all substrates dissociated slowly from the RNase H site of RT. The steady state rates of RNA cleavage (0.04 ± 0.01 s^{-1}) with all substrates (Table 1) are close to value of 0.06 s^{-1} obtained by Kati *et al.* (1992) and the value of 0.04 s^{-1} based upon kinetic analysis of single nucleotide incorporation using the 37/66-mer (Suo & Johnson, 1997a). These measurements also agree with the dissociation rate estimated using a DNA trapping experiment (0.042 s^{-1}) with the 48/66-mer (Suo & Johnson, 1997a). This suggests

that subsequent turnovers of RNA cleavage, like DNA polymerization with linear templates, are limited by the dissociation from the enzyme of products of single nucleotide incorporation reactions or single hydrolysis events. The steady state rates in Table 1 indicate that all substrates dissociate slowly from the RNase H active site of RT. Table 1 also shows that the burst rates representing the RNA cleavage rates vary with different primers. The reason for these differences is unclear, but may reflect some nucleotide sequence specificity of the RNase H activity.

The burst amplitudes provide a measurement of the fraction of enzyme molecules productively bound by substrates at the RNase H site. This amplitude varied from 30 to 70% with different primers (Table 1). This variation is not as large as that seen for the reaction amplitudes of nucleotide incorporations in the fast phase (Suo & Johnson, 1997a). Thus, the RNA secondary structure affects the substrate binding at the RNase H active site to a lesser extent than at the polymerase site of RT. The same conclusion has been drawn from the binding affinity data of Table 2 in Suo and Johnson (1997a).

It is noteworthy that the amplitudes of the RNA cleavage reactions observed with 32/66-mer, 35/66-mer, 36/66-mer, and 48/66-mer substrates are larger than the corresponding reaction amplitudes of nucleotide incorporations in the fast phase. This suggests that a large portion of substrates at the pause sites bound to the RNase H site productively while they were simultaneously bound nonproductively at the polymerase site of RT. This observation is consistent with our conclusion that the dangling end at the base of the hairpin forces the 3′ end of primer away from the polymerase site and shifts the location of the RNase H cleavage. Indeed, the burst amplitude of RNA cleavage with the 48/66-mer is highest among all substrates (Table 1) providing additional support for the conclusion that one nucleotide dangling end and the hairpin structure of 48/66-mer do not significantly affect the binding of the 48/66-mer to RT.

RNase H Activity of RT Is Not Important for RT to Read through RNA Secondary Structure. The possible role of RNase H activity on RNA secondary structure melting was examined by the same processivity experiment at 37 °C with the RNase H deficient mutant D443N. The product accumulation pattern shown in Figure 4 is very similar to the one generated by wt-RT shown in Figure 2 in Suo and Johnson (1997b). This suggests that the RNase H activity does not facilitate RT to traverse the RNA hairpin structure of our template. Dudding *et al.* (1991) have reported that mutant D443N and wt-RT shared pause sites when catalyzing primer extension along a 345 nucleotide template derived from the *gag* region of HIV-1 RT. We have used *Mfold* program to predict that all of these pause sites except two sites are at the stems of hairpin structure (Suo & Johnson, 1997b). These two sites are at runs of template rAs and rUs where mutant RT D443N paused significantly longer (Dudding *et al.*, 1991). These results suggest that the RNase H activity is not critical for RT to read through RNA secondary structure although it facilitates DNA synthesis through the runs of rAs and rUs.

Searching for Accessory Proteins To Increase RT Processivity. Before RT reached the RNA secondary structure of our RNA template, the average processivity was estimated to be about 10 in the three dATP incorporations (Suo & Johnson, 1997a). The processivity of RT was reduced to approximately 1 while reading through the template secondary structure because of the strong pausing at several positions. It is possible, but not essential, that HIV-1 RT may recruit a helicase-like accessory protein to increase its processivity when it traverses RNA template secondary structure. Alternatively, the binding of the nucleocapsid protein to the RNA may facilitate its unwinding. However, in our tests of the effect of the nucleocapsid protein on unwinding, we only saw inhibition of DNA elongation. The intermediate product accumulation pattern is similar to Figure 2 in Suo and Johnson (1997b) except that product 29-mer accumulated more than other intermediates in the first 6 s. In the absence of nucleocapsid protein, the 29-mer did not accumulate after 0.3 s in Figure 2 of Suo and Johnson (1997b). Since one nucleocapsid molecule was found to bind seven nucleotides (You & McHenry, 1993), this corresponds well with the length of the single-stranded linker between the 3′ terminus of primer and the beginning of the template hairpin suggesting that the nucleocapsid protein inhibits polymerization by binding to this linker. The reason for 29-mer accumulation is unclear. It is possible that some nucleocapsid molecules bind part of the linker and the hairpin stem and therefore forced RT to pause. The accumulation patterns of other intermediate products in the presence and absence of nucleocapsid are similar. This suggests that the nucleocapsid did not accelerate the melting of RNA secondary structure. Ji *et al.* (1996) reported that addition of nucleocapsid to RT·DNA·dNTP ternary complexes slightly increased the processivity of RT at specific DNA template sites with potential secondary structures. We used the same addition order and did not find the same processivity change with our RNA template. Although nucleocapsid was demonstrated to unwind some specific secondary structures (Khan & Giedroc, 1992; Tsuchihashi & Brown, 1994; You & McHenry, 1994), our results suggest that it is not the accessory protein which RT recruits to increase its processivity.

RT may recruit DNA and RNA helicases from host cells to improve its processivity. RNA helicase A and RNA helicase II from HeLa cells catalyze the unwinding of duplex RNA utilizing nucleoside triphosphates as their energy source (Lee *et al.*, 1992; Flores-Rozas & Hurwitz, 1993). They were tested separately with our RNA template, and we found that they had no effect on RT processivity. We also examined T7 DNA helicase (Patel *et al.*, 1992) and *E. coli* thioredoxin (Huber et al., 1987) individually with the DNA template, an analog of our RNA template and it also did not improve RT processivity. So far, no accessory protein has been found to dramatically increase the processivity of HIV-1 RT. However, our results have demonstrated that HIV-1 RT facilitates the RNA secondary structure switching (Suo & Johnson, 1997b), which acts as a helicase to help RT to read through RNA secondary structure. Additionally, it has been reported that HIV-1 RT alone is able to catalyze the synthesis of several hundred nucleotide DNA products at the rate of about 1−3 nucleotides per second *in vitro* using both DNA and RNA templates derived from HIV-1 genome (Klarmann *et al.*, 1993), which agrees with the estimated overall rate of viral DNA synthesis *in vivo* (Klarmann *et al.*, 1993). These studies suggest that HIV-1 RT may not require an accessory protein to complete viral DNA replication. Moreover, RT is present in greater molar excess than the single-stranded RNA genome in HIV virus (Hottiger &

Hubscher, 1996), and the data presented here show that RT facilitates the unwinding of the RNA hairpin during the process of DNA polymerization.

In summary, we studied the effect of RNA secondary structure on RNase H activity of HIV-1 RT. We demonstrated that specific RNA cleavage products accumulated along with DNA polymerization products. The strong correlation between the accumulated RNA cleavage products and DNA products suggests that RNase H activity is coordinated with the polymerase activity by the movement of the enzyme along the template driven by the polymerization process. No other higher order cooperativity exists between the two active sites. RNase H activity acts primarily as an endonuclease. It also has an apparently slower 3′ → 5′ exonuclease activity, which cleaves RNA further when elongation stops. The polymerase and RNase H active sites were separated by a fixed distance corresponding to 19 base pairs of DNA/RNA heteroduplex when RT traversed a large template secondary structure. The nonproductive binding of substrates at the polymerase site provides a rationale for the increase in observed distance between the 3′ termini of DNA primer and major RNA cleavage site at specific sites. The pre-steady-state kinetic analysis of RNA cleavage indicates that all substrates dissociate slowly from the RNase H site or the binding cleft of RT and that most of the strongly accumulated DNA/RNA duplexes bound nonproductively at the polymerase site but still bound productively at the RNase H site. That similar processive polymerization catalyzed by wild-type and the RNase H-deficient mutant RT (D443N) demonstrated that RNase H activity is not critical for RT to synthesize DNA through RNA secondary structure. HIV-1 nucleocapsid inhibited DNA elongation by blocking the binding of RT to substrates.

ACKNOWLEDGMENT

We sincerely thank Dr. Roger Goody (Max-Planck Institute, Heidelberg) for providing the clones of the p66(WT) and p51(WT) subunits, Dr. Charles S. McHenry (University of Colorado Health Sciences Center) for providing HIV-1 nucleocapsid protein (NCp7), Dr. Jerard Hurwitz (Sloan-Kettering Institute, NY) for providing RNA helicase A and II from HeLa cells, and Dr. Kevin Hecker (Pennsylvania State University) for providing T7 DNA helicase.

REFERENCES

Champoux, J. J. (1993) in *Reverse Transcriptase* (Skalka, A. M., & Goff, S. P., Eds.) pp 103−117, Cold Spring Harbor Laboratory Press, Plainview, NY.

DeStefano, J. J., Buiser, R. G., Mallaber, L. M., Bambara R. A., & Fay, P. J.(1991) *J. Biol. Chem. 266*, 24295−24301.

Dudding, L. R., Nkabinde, N. C., & Mizrahi, V. (1991) *Biochemistry 30*, 10498−10506.

Flores-Rozas, H., & Hurwitz, J. (1993) *J. Biol. Chem. 268*, 21372−21383.

Furfine, E. S., & Reardon, J. E. (1991) *J. Biol. Chem. 266*, 406−412.

Hansen, J., Schulze, T., & Moelling, K. (1987) *J. Biol. Chem. 262*, 12393−12396.

Hermann, T., Meier, T., Götte, M., & Heumann, H. (1994) *Nucleic Acids Res. 22*, 4625−4633.

Hottiger, M., & Hubscher, U. (1996) *Biol. Chem. Hoppe-Seyler 377*, 97−120.

Huber, H. E., Tabor, S., & Richardson, C. C. (1987) *J. Biol. Chem. 262*, 16224−16232.

Huber, H. E., McCoy, J. M., Seehra, J. S., & Richardson, C. C. (1989) *J. Biol. Chem. 264*, 4669−4678.

Jacobo-Molina, A., Ding, J., Nanni, R. G., Clark, A. D., Jr., Lu, X., Tantillo, C., Williams, R. L., Kamer, G., Ferris, A. L., Clark, P., Hizi, A., Hughes, S. H., & Arnold, E. (1993) *Proc. Natl. Acad. Sci. U.S.A. 90*, 6320−6324.

Ji, X., Klarmann, G. J., & Preston, B. D. (1996) *Biochemistry 35*, 132−143.

Kati, W. M., Johnson, K. A., Jerva, L. F., & Anderson, K. S. (1992) *J. Biol. Chem. 267*, 25988−25997.

Khan, R., & Giedroc, D. P., (1992) *J. Biol. Chem. 267*, 6689−6695.

Kim, S., Bryn, R., Groopman, J., & Baltimore, D. (1989) *J. Virol. 63*, 3708−3713.

Klarmann, G., Schauber, C. A., & Preston, B. D., (1993) *J. Biol. Chem. 268*, 9733−9802.

Kohlstaedt, L. A., Wang, J., Friedman, J., Rice, P. A., & Steitz, T. A. (1992) *Science 256*, 1783−1790.

Krug, M. S., & Berger, S. L. (1989) *Proc. Natl. Acad. Sci. U.S.A. 86*, 3539−3543.

Lee, C., & Hurwitz, J. (1992) *J. Biol. Chem. 267*, 4398−4407.

Mizrahi, V., Usdin, M. T., Harington, A., & Dudding, L. R. (1990) *Nucleic Acids Res. 18*, 5359−5363.

Muller, B., Restle, T., Weiss, S., Gautel, M., Sczakiel, G., & Goody, R. S. (1989) *J. Biol. Chem. 264*, 13975−13978.

Patel, P. H., Jacobo-Molina, A., Ding, J., Tantillo, C., Clark, A. D., Jr., Raag, R., Nanni, R. G., Hughes, S. H., & Arnold, E. (1995) *Biochemistry 34*, 5351−5363.

Patel, S. S., Rosenberg, A. H., Studier, F. W., & Johnson, K. A. (1992) *J. Biol. Chem. 267*, 15013−15021.

Rodgers, D. W., Gamblin, S. J., Harris, B. A., Ray, S., Culp, J. S., Hellmig, B., Woolf, D. J., Debouck, C., & Harrison, S. C. (1995) *Proc. Natl. Acad. Sci. U.S.A. 92*, 1222−1226.

Sanger, F., Niklen, S., & Coulson, A. R. (1977) *Proc. Natl. Acad. Sci. U.S.A. 74*, 5463−5467.

Schatz, O., Mous, J., & Le Grice, S. F. J. (1990) *EMBO J. 9*, 1171−1176.

Suo, Z., & Johnson, K. A. (1997a) *Biochemistry 36*, 12459−12467.

Suo, Z., & Johnson, K. A. (1997b) *Biochemistry* (manuscript submitted for publication).

Tsuchihashi, Z., & Brown, P. (1994) *J. Virol. 68*, 5863−5870.

Wöhrl, B. M., & Moelling, K. (1990) *Biochemistry 29*, 10141−10147.

Wöhrl, B. M., Tantillo, C., Arnold, E., & Le Grice, S. F. J. (1995) *Biochemistry 34*, 5343−5350.

You, J. C., & McHenry, C. S. (1993) *J. Biol. Chem. 268*, 16519−16527.

You, J. C., & McHenry, C. S. (1994) *J. Biol. Chem. 269*, 31491−31495.

BI971218+